JOURNAL OF VIROLOGY, Sept. 1994, p. 5365–5374
0022-538X/94/$04.00+0

Vol. 68, No. 9

The Size and Symmetry of B Capsids of Herpes Simplex Virus Type 1 Are Determined by the Gene Products of the UL26 Open Reading Frame

PRASHANT DESAI,[1] SIMON C. WATKINS,[2] AND STANLEY PERSON[1]*

Department of Molecular Genetics and Biochemistry[1] and Department of Cell Biology and Physiology,[2] University of Pittsburgh Medical School, Pittsburgh, Pennsylvania 15261

Received 28 March 1994/Accepted 1 June 1994

Herpes simplex virus type 1 (HSV-1) B capsids are composed of seven proteins, designated VP5, VP19C, 21, 22a, VP23, VP24, and VP26 in order of decreasing molecular weight. Three proteins (21, 22a, and VP24) are encoded by a single open reading frame (ORF), UL26, and include a protease whose structure and function have been studied extensively by other investigators. The protease encoded by this ORF generates VP24 (amino acids 1 to 247), a structural component of the capsid and mature virions, and 21 (residues 248 to 635). The protease also cleaves C-terminal residues 611 to 635 of 21 and 22a, during capsid maturation. Protease activity has been localized to the N-terminal 247 residues. Protein 22a and probably the less abundant protein 21 occupy the internal volume of capsids but are not present in virions; therefore, they may form a scaffold that is used for B capsid assembly. The objective of the present study was to isolate and characterize a mutant virus with a null mutation in UL26. Vero cells were transformed with plasmid DNA that encoded ORF UL25 through UL28 and screened for their ability to support the growth of a mutant virus with a null mutation in UL27 (K082). Four of five transformants that supported the growth of the UL27 mutant also supported the growth of a UL27-UL28 double mutant. One of these transformants (F3) was used to isolate a mutant with a null mutation in UL26. The UL26 null mutation was constructed by replacement of DNA sequences specifying codons 41 through 593 with a *lacZ* reporter cassette. Permissive cells were cotransfected with plasmid and wild-type virus DNA, and progeny viruses were screened for their ability to grow on F3 but not Vero cells. A virus with these growth characteristics, designated KUL26ΔZ, that did not express 21, 22a, or VP24 during infection of Vero cells was isolated. Radiolabeled nuclear lysates from infected nonpermissive cells were layered onto sucrose gradients and subjected to velocity sedimentation. A peak of radioactivity for KUL26ΔZ that sedimented more rapidly than B capsids from wild-type-infected cells was observed. Sodium dodecyl sulfate-polyacrylamide gel electrophoresis analysis of the gradient fractions showed that the peak fractions contained VP5, VP19C, VP23, and VP26. Analysis of sectioned cells and of the peak fractions of the gradients by electron microscopy revealed sheet and spiral structures that appear to be capsid shells. Therefore, 22a and perhaps the less abundant 21 form a scaffold that is essential for B capsid formation and its icosahedral symmetry. Since several bacteriophages employ a scaffold to determine capsid size and shape, it appears that HSV-1 uses the same principles for capsid assembly and maturation. The size and symmetry of HSV-1 capsids must require the interaction of 22a and perhaps 21 with one or more of the remaining four components of the capsids. In related experiments a thiol-cleavable cross-linking reagent, dithiobis(succinimidylpropionate), was used to test for cross-links in the molecules that make up B capsids. Protein 22a formed cross-links to itself and to VP5 and VP19C, which may be indicative of the interactions required for the icosahedral symmetry of HSV-1 capsids. Cross-links were also detected between VP5, VP19C, and VP23. Null mutant viruses for VP5 or VP23 do not form recognizable structures in nonpermissive cells, and the mutants retain the protease-processing activity associated with the UL26 gene product. Although the enzyme activity of the UL26 gene product may be independent of capsid structure, the location of VP24 and 21 within wild-type capsids suggests a role for the protease in capsid maturation.

The herpes simplex virus type 1 (HSV-1) B capsid is composed of seven capsid proteins. They are designated, in order of decreasing molecular masses, VP5 (150 kDa), VP19C (52 kDa), 21 (47 kDa), 22a (40 kDa), VP23 (33 kDa), VP24 (25 kDa), and VP26 (12 kDa) (5, 16, 19). All except 21 and VP24 are present at approximately 500 to 1,500 copies per capsid. Proteins 21 and VP24 are less abundant and are present at approximately 150 molecules per capsid (see, for example, reference 33). VP5 is the major capsid protein, makes up approximately 60% of the capsid mass, and forms the hexons and pentons present in capsids (30, 31, 45).

* Corresponding author. Phone: (412) 648-9097. Fax: (412) 624-1401.

Three types of capsids can be isolated from HSV-1 infected cells. They are visualized as light-scattering bands in sucrose gradients and are designated A, B, and C, in order of increasing distance sedimented (16). They differ in protein and DNA composition and in their eventual fate in the infected cell. A and C capsids are similar in protein content, but only C capsids contain a genomic equivalent of DNA and hence mature into infectious virions. Protein 22a is present only in B capsids and occupies the inner capsid space (1, 28, 29, 38). It is probable that homologs of 22a will be found in all herpesviruses, which implies a common function in capsid assembly (47, 48). Gibson et al. (15) were the first to suggest that this class of herpesvirus proteins may function as a scaffold for assembly of the capsid shell.

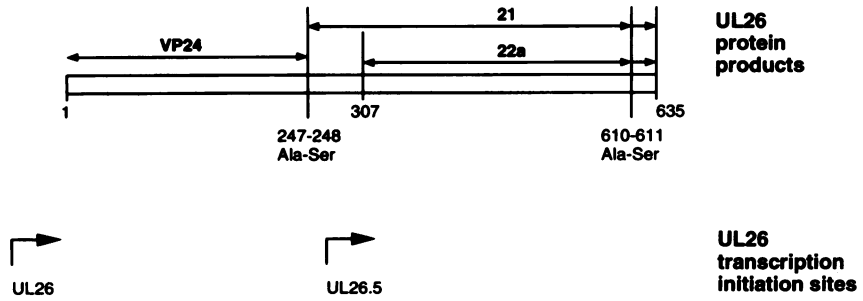

FIG. 1. Genetic organization of the UL26 ORF. Three of the seven capsid proteins, VP24, 21, and 22a, are encoded by a single ORF. The minor transcript, UL26, encodes a 635-residue protease that cleaves between residues 247 and 248 to release VP24 and 21. Protein 22a is encoded by the major transcript, UL26.5, and translation initiation of 22a occurs at residue 307. Both 21 and 22a are cleaved by the protease between residues 610 and 611. The positions of the alanine-serine cleavage sites and of the transcription initiation sites are shown. Proteins 21 and 22a are also commonly referred to as members of the ICP35 family.

The open reading frame (ORF) that specifies each capsid protein has now been assigned, and all map to the unique long (UL) region of the HSV-1 genome (26; see also reference 33). Three of the seven capsid proteins are encoded by a single ORF, designated UL26 (Fig. 1). Two transcripts have been mapped to the UL26 ORF that are in the same reading frame and are 3′ coterminal (20, 23). One transcript, designated UL26, is initiated 180 nucleotides upstream of the entire coding sequence, and the second, more abundant transcript, designated UL26.5, is initiated near the center of the ORF (1,000 nucleotides downstream of the first transcript). The UL26 ORF (635 amino acid residues) encodes a protease (25, 36), and cleavage occurs at two sites, a maturation site between residues 610 and 611 and a release site between residues 247 and 248 (12). The proteolytic activity specified by UL26 has been localized to the N-terminal 247 residues (24, 46). The products of the release site cleavage generate B capsid proteins VP24 and 21 (46). On the basis of amino acid sequence determination, VP24 was assigned to the N terminus of UL26 (residues 1 to 247) (6), and the N terminus of 21 was shown to be amino acid 248 and extended to the end of the UL26 ORF (33). The more abundant 22a is encoded by the UL26.5 transcript and is initiated at codon 307 (23, 25). Therefore, 21 and 22a are identical in amino acid sequence between residues 307 and 635. Since 22a (17) and probably 21 are not virion proteins, they are not designated here with a VP (virion protein) prefix (43). Proteins 21 and 22a are phosphorylated, and their multiple forms, analyzed by sodium dodecyl sulfate-polyacrylamide gel electrophoresis (SDS-PAGE) before and after cleavage at the maturation site, have commonly been referred to as ICP35 family a to f since they were identified by antibody precipitation from infected-cell extracts and revealed at least six bands on SDS-PAGE (2). The gene products of the UL26 ORF homolog for simian cytomegalovirus have been extensively characterized by Gibson and colleagues (see, for example, references 47 and 48).

In the study reported here, a transformed cell line that expressed the gene products of the UL26 ORF was isolated. The cell line was used to isolate a mutant virus with a null mutation in UL26, which does not synthesize 21, 22a, or VP24. Following infection of nonpermissive cells, the remaining capsid proteins (VP5, VP19C, VP23, and VP26) interact to form sheets or spirals of capsid shells that lack the normal icosahedral symmetry found in B capsids (49). Therefore, HSV-1 capsid formation and maturation utilize 22a and perhaps 21 to form a scaffold that confers on B capsids the correct size and shape.

MATERIALS AND METHODS

Cells and viruses. Human embryonic lung (HEL) cells were grown and maintained as described by Person et al. (32). Vero cells and transformed cell lines were grown in Eagle's minimal essential medium supplemented with 10% fetal calf serum (Gibco-BRL) and passaged as for HEL cells. Virus stocks of KOS (HSV-1), of KΔ4BX, and of K082, K5ΔZ, K23Z, and KUL26ΔZ null mutants were prepared as previously described (32). F3 was used as the permissive cell line for the propagation of the UL26 null mutant and gave yields of approximately 200 PFU per cell.

Plasmids. pKEF-B5 contains a 12.4-kb DNA fragment of the KOS genome (map units 0.315 to 0.397) cloned into pBR325 (8) and encodes the ORF of UL25 through UL28 (see Fig. 2). The 6.5-kb *Not*I fragment derived from pKEF-B5 was cloned into the *Not*I site of the 3.0-kb pBluescript II KS(−) vector (Stratagene). The *Bam*HI site of the vector was deleted prior to the insertion of the *Not*I fragment. A 1.7-kb deletion was generated within the *Not*I fragment by digestion with *Bam*HI (the d′ and e′ fragments of *Bam*HI-digested HSV-1 DNA), and the *lacZ* gene derived as a *Bam*HI cassette from pSC8 (4) was then cloned into the *Bam*HI site. This cassette does not contain an initiation codon but does have a TAA termination codon. *Bam*HI cleaves the UL26 ORF between codons 40 and 41 and cleaves the 5′ end of the *lacZ* cassette between codons 7 and 8. Ligation of these two sequences through this cleavage site maintains the UL26 reading frame such that the LacZ polypeptide is synthesized fused to the first 40 residues of the UL26 ORF.

Construction of transformed Vero cell lines. The procedure of DeLuca et al. (9) was followed for transformation of Vero cells. Subconfluent monolayers of Vero cells (2×10^6 cells) in 100-mm petri dishes were cotransfected with pSV2neo (1.0 μg) (42) and pKEF-B5 (9 and 15 μg) by the calcium precipitation procedure of Graham and van der Eb (18). At 24 h after transfection the cells were harvested and plated at a density of 4×10^5 cells per 100-mm dish in medium containing 1 mg of G418 (Gibco-BRL) per ml. The medium was replenished every 3 days. G418-resistant colonies were harvested by using Perspex cloning chambers and tested for their ability to support the replication of K082, a glycoprotein B null mutant specified by the UL27 ORF (3). One such cell line, designated F3, was chosen for the isolation of the UL26 null mutant.

Marker transfer of null mutations. Subconfluent monolayers of F3 cells in 60-mm dishes were cotransfected with 2 μg of linearized plasmid and 5 μg of KOS genomic DNA extracted

from crude virion preparations as described previously (10). When foci were observed (48 h after transfection), the cell monolayers were harvested, frozen and thawed once, and sonicated, and the titer of the total virus progeny was determined. Initially, attempts were made to isolate viruses that contained the UL26 deletion-*lacZ* insertion by using the Bluo-gal overlay assay (10). However, because of the weak signal of the *lacZ* gene expression (presumably as a result of the weak UL26 promoter), recombinant viruses were instead isolated by screening single-plaque isolates on Vero and F3 cells. Viruses that formed plaques on F3 cells but not on Vero cells were further characterized. One such isolate was plaque purified three times and designated KUL26ΔZ. This virus forms light blue plaques in the Bluo-gal overlay assay.

Southern blot hybridization. DNA sequences were detected after agarose gel electrophoresis as described by Southern (41), using random-primer-labeled probes (13).

Radiolabeling, immunoprecipitation, and SDS-PAGE. Infected cells were radiolabeled by using preformed monolayers in six-well trays (35-mm-diameter wells). Infected-cell monolayers were rinsed twice with Tricine-buffered saline (32) and overlaid with methionine-free Dulbecco's modified Eagle's medium containing 100 μCi of [^{35}S]methionine. The cells were lysed in 1.0 ml of RIPA buffer (50 mM Tris [pH 7.2], 150 mM NaCl, 1% sodium deoxycholate, 1% SDS, 1% Triton X-100) plus 0.5 mM tosyl-lysyl-chloromethyl ketone (TLCK). Lysates were clarified by centrifugation at 34,000 rpm for 30 min at 4°C in a Beckman SW55 Ti rotor. Total-infected-cell polypeptides were examined after the samples were boiled in 2× Laemmli sample buffer. For immunoprecipitation of antigen, 250 μl of the lysate was combined with 3 μl of antibody and incubated overnight at 4°C. The next day, 50 μl of protein A-Sepharose beads (Sigma) swollen in RIPA buffer was added to the tube, and the mixture was incubated for 2 h at 4°C with continuous rotation. The beads were washed five times with RIPA buffer and resuspended in 25 μl of 2× Laemmli sample buffer. Samples (10 μl) were boiled prior to electrophoresis. SDS-PAGE analyses were performed by using the mini-protean gel system (Bio-Rad), unless otherwise stated. Gels were cast by following the supplier's protocol except that *N,N'*-diallytartardiamide (DATD) was used as the cross-linking agent. Gels were treated with En^{3}Hance (NEN-DuPont) and dried prior to autoradiography.

Sedimentation analysis. Sedimentation analysis of radiolabeled nuclear extracts derived from infected HEL cells was performed as described by Desai et al. (10).

Chemical cross-linking of capsids. [^{35}S]methionine-labeled B capsids isolated by purification through sucrose gradients (33) were treated to various concentrations (0.0123 to 0.333 mg/ml) of the homobifunctional reversible cross-linker dithiobis(succinimidylpropionate) (DSP; span size, 12 Å [1.2 nm]) obtained from Pierce Co. Stock solutions of the cross-linker (10 mg/ml) in dimethyl sulfoxide were made just before use. The cross-linker was diluted into HN buffer (25 mM *N*-2-hydroxyethylpiperazine-*N'*-2-ethanesulfonic acid [HEPES; pH 8.0], 30 mM NaCl) to give the final working concentration. All cross-linking reactions were performed with HN buffer. The reaction was allowed to proceed for 30 min at room temperature, and then Tris base was added to a final concentration of 100 mM to quench the reaction.

Two-dimensional gel electrophoresis. Cross-linked capsid proteins were resolved in the first dimension under nonreducing conditions in a 4 to 15% mini-protean gradient gel. Samples were boiled in Laemmli sample buffer which did not contain dithiothreitol or 2-mercaptoethanol before electrophoresis. Gel slices of the first dimension were soaked in reducing buffer (50 mM Tris [pH 6.8], 1% SDS, 1% 2-mercaptoethanol) for 15 min at 65°C prior to electrophoresis in the second dimension. Gel slices were inserted into the stacking gel of a 17% gel, sealed with agarose, and electrophoresed.

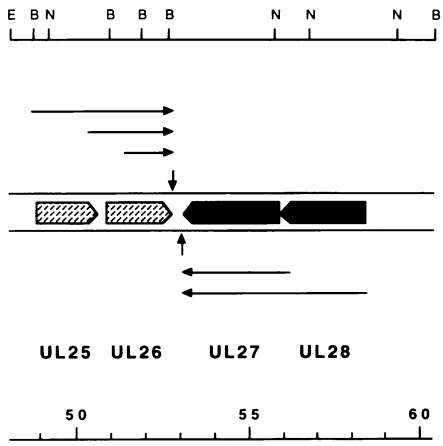

FIG. 2. The map unit 0.315 to 0.397 region of the KOS genome. The 12.4-kb fragment (KEF-B5) was generated by partial *Bam*HI digestion of the *Eco*RI F fragment of KOS DNA previously cloned into pBR325. Restriction sites are shown in the top line for *Bam*HI (B), *Eco*RI (E), and *Not*I (N). The remainder of the figure is from sequence analysis of HSV-1 17 (27). ORFs and directions of translation are as indicated, as are transcripts (←) and polyadenylation signals (↑). The pKEF-B5 plasmid specifies genes UL25 through UL28. Nucleotide numbers from the left end of the strain 17 genome are given at the bottom of the figure in kilobases.

RESULTS

Isolation of a transformed cell line that expresses the UL26 proteins. UL26 encodes three proteins (designated 21, 22a, and VP24), and the mapping of a temperature-sensitive lesion to this ORF (35) implies that one or more of these proteins specify an essential function for capsid assembly. Therefore, to isolate mutants with null mutations in this ORF, a transformed cell line that expresses these proteins in *trans* is required. Vero cells were cotransfected with pSV2neo and pKEF-B5 (Fig. 2), which specifies genes UL25 to UL28. It was shown previously that Vero cells transformed with HSV-1 DNA that encoded adjacent genes expressed both gene products (10). A similar strategy was used in the present study. Colonies that were resistant to the drug G418 were harvested and tested for their ability to complement K082, a null mutant of UL27. K082 contains a polypeptide chain termination codon as a result of *Hpa*I linker insertion within codon 43 of the glycoprotein B (gB) gene adjacent to UL26 (3). Thirty-seven G418-resistant stable transformants were isolated, and five of them gave the plating efficiencies for K082 shown in Table 1. F3, F12, and B8 gave efficiencies that were similar to those of the D6 cell line, isolated earlier to support the growth of gB mutants (3), and F11 and F17 gave significantly lower efficiencies. These transformed cell lines were also tested for their ability to support the growth of a double-deletion mutant virus (KΔ4BX) (11). This virus contains a deletion in UL27 (gB) that extends into the neighboring UL28 (ICP18.5) gene. All of the transformed cell lines, except F12 (which gave no plaques), gave plating efficiencies that were similar to those for K082. F3 gave virus yields for the growth of K082 that were similar to those obtained with D6 cells (data not shown), and it was used in

TABLE 1. Titers of the gB null mutant virus, K082, on transformed Vero cell lines

Cell line	Virus titer (PFU/ml)	% of titer on D6
D6	3.2×10^8	100
F11	2.1×10^8	67
F12	3.7×10^8	114
F17	1.1×10^8	34
B8	3.1×10^8	95
F3	3.1×10^8	96

experiments in an attempt to isolate a null mutation in the UL26 gene.

Construction and isolation of a mutant with a null mutation in UL26. The goal of these experiments was to construct a null mutation in the UL26 gene and transfer the mutation to the KOS genome by using the F3 transformed cell line as host. The UL26 specifies three capsid proteins, and we attempted to isolate a virus deleted for all of the genes. The *Not*I fragment that encodes UL26 (Fig. 2) was cloned into a vector whose *Bam*HI site had been deleted previously. The d′ and e′ *Bam*HI fragments within UL26 (codons 41 through 593) were deleted and replaced with a *lacZ* cassette (4). The resulting plasmid (pKUL26ΔZ) was linearized and used with KOS DNA to cotransfect F3 cells. Progeny viruses were harvested and assayed for their ability to form plaques on F3 but not on Vero cells. A virus, designated KUL26ΔZ, with these properties was plaque purified twice before further characterization. The ability to isolate a putative UL26 null mutation on F3 cells implies that this cell line expresses UL26 in addition to the UL27 and UL28 gene products.

To confirm the introduction of the plasmid-specified mutation into virus, we prepared small batches of viral DNA from infected cells and analyzed them by Southern blot hybridization (Fig. 3). In KUL26ΔZ, a deletion of 1.7 kb was created and was followed by the addition of the 3-kb *lacZ* fragment. This results in an overall insertion of 1.3 kb. The presence of an *Eco*RI site in the *lacZ* gene results in the cleavage of the *Eco*RI F fragment (16.1 kb) of KOS (lane 1) into 11.4- and 6.0-kb fragments in the mutant (lane 2), of which only the 6.0-kb fragment hybridizes to the probe (see the diagram at the bottom of Fig. 3). For KOS DNA restricted with *Bam*HI, the probe hybridizes to fragments that are 2.3 kb (*Bam*HI-U), 0.86 kb (*Bam*HI-d′), and 0.8 kb (*Bam*HI-e′) in size (lane 3). Of these fragments, only the BamHI U fragment hybridizes to the probe, since the *Bam*HI d′ and e′ fragments are deleted in KUL26ΔZ viral DNA (lane 4).

Phenotypic characterization of the UL26 null mutant. The plating efficiencies of KOS, K082, and KUL26ΔZ were tested on the various pKEF-B5-transformed cell lines (Table 2). Four of the five transformed cell lines supported the growth of the UL26 null mutant virus; the fifth (F12) did not. This cell line similarly did not support the growth of a lesion in UL28. The remaining four cell lines gave similar plating efficiencies for viruses deleted in either UL26, UL27, or UL28. The cell lines were not tested for the expression of the remaining ORF present in pKEF-B5 (UL25). The percentage of wild-type virus in the KUL26ΔZ stock used for this study was 0.0014%. Wild-type virus detected in the mutant virus stocks is due to recombination that occurs between homologous sequences present in the mutant viral genome and the resident wild-type sequence in the transformed cell line.

The next series of experiments were carried out to examine viral protein synthesis in extracts derived from mutant-infected

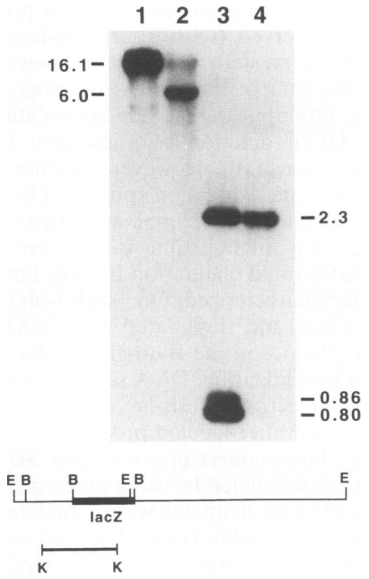

FIG. 3. Southern blot analysis of the UL26 null mutant. DNA (2 μg) extracted from KOS-infected Vero cells (lanes 1 and 3) and KUL26ΔZ-infected F3 cells (lanes 2 and 4) was digested with restriction endonucleases *Eco*RI (lanes 1 and 2) and *Bam*HI (lanes 3 and 4). The resulting restriction fragments were separated on a 1% agarose gel and transferred to nitrocellulose membranes. Filters were hybridized to a ^{32}P-labeled probe that specifies the *Kpn*I T sequences. Shown at the bottom of the figure is a representation of the *Eco*RI F region of KUL26ΔZ, and the *Kpn*I T fragment of KOS DNA. The *Bam*HI d′ and e′ fragments of KOS DNA were deleted in the construction of the mutant virus prior to the insertion of the *lacZ* gene at the remaining *Bam*HI site. Restriction enzyme sites correspond to *Eco*RI (E), *Bam*HI (B), and *Kpn*I (K).

nonpermissive cells. Vero and F3 cells were infected with KOS and KUL26ΔZ at a multiplicity of infection (MOI) of 10 PFU per cell and metabolically labeled with [^{35}S]methionine from 9 to 10 h postinfection. Total infected-cell polypeptides were examined by SDS-PAGE (Fig. 4). Results are shown for KOS- and KUL26ΔZ-infected Vero (lanes 2 and 3) and F3 (lanes 5 and 6) cells, respectively. KUL26ΔZ synthesizes wild-type levels of infected-cell proteins under nonpermissive conditions, except for a 40-kDa polypeptide (indicated by an open circle to the left of lanes 2 and 5). This polypeptide is present in lysates prepared from mutant-infected F3 cells at levels that are approximately one-half of those present in wild-type infections (compare lanes 2 and 5 with lane 6). The 80-kDa polypeptide

TABLE 2. Titers of wild-type, K082, and KUL26ΔZ viruses on transformed Vero cell lines

Cell line	Titer (PFU/ml) of:		
	KOS	K082	KUL26ΔZ
Vero	1.2×10^9	0[a]	0[b]
D6	1.1×10^9	3.2×10^8	0[b]
F11	4.1×10^8	2.1×10^8	6.6×10^9
F12	1.2×10^9	3.8×10^8	0[b]
F17	1.8×10^8	1.2×10^8	1.9×10^9
B8	9.7×10^8	3.4×10^8	7.0×10^9
F3	9.9×10^8	3.2×10^8	7.7×10^9

[a] No plaques produced at the 1×10^7 dilution factor.
[b] No plaques produced at the 1×10^8 dilution factor.

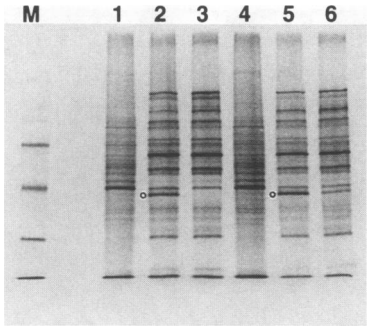

FIG. 4. Synthesis of viral polypeptides in KUL26ΔZ-infected cells. Vero cells (lanes 1 to 3) and F3 cells (lanes 4 to 6) were infected at an MOI of 10 PFU per cell with KOS (lanes 2 and 5) or KUL26ΔZ (lanes 3 and 6) or were mock infected (lanes 1 and 4). Cells were metabolically labeled with [^{35}S]methionine from 9 to 10 h after infection. Lysates prepared from the cells were electrophoresed by SDS-PAGE (12% polyacrylamide). Protein standards in order of decreasing molecular masses (69, 46, and 30 kDa) are shown in lane M. The position of the 40-kDa ICP35 polypeptide is marked by an open circle to the left of lanes 2 and 5.

is produced in quantities that are too low to be visualized in the total infected-cell lysates. However, antibodies specific for the UL26 and UL26.5 gene products precipitated 40- and 80-kDa polypeptides from KOS-infected Vero cells and KUL26ΔZ-infected F3 cells but not from KUL26ΔZ-infected Vero cells (data not shown).

Sedimentation analysis of the UL26 null mutant. To determine if capsid precursors accumulate in nonpermissive cells, we analyzed nuclear extracts of KUL26ΔZ-infected cells following sedimentation through sucrose gradients. For this purpose, HEL cells were used as the nonpermissive cells. Cell monolayers were infected with KOS or the mutant viruses and labeled with [^{35}S]methionine from 8 to 24 h postinfection. K23Z, a null mutant virus for the VP23 capsid protein, which was shown previously not to produce capsid precursor structures, was included as a negative control. Nuclear lysates were prepared and layered onto 20 to 50% sucrose gradients. After sedimentation, fractions were collected and analyzed by SDS-PAGE (Fig. 5). Two peaks of radioactivity were observed for KOS-infected cells (Fig. 5A), corresponding to the faster-sedimenting C capsids (fraction 12) and the empty B capsids (fractions 7 through 9). Both B and C capsids contain VP5, VP19C, VP23, VP24, and VP26. Proteins 22a and 21 are detected only in B capsids, as expected. In addition to the known capsid proteins, several bands are routinely detected in the region between VP5 and VP19C, and one or more of these could be viral proteins. Sedimentation analysis of the K23Z mutant lysate (Fig. 5C) does not reveal any cosedimenting capsid proteins in any of the fractions, as previously shown (10). However, for the UL26 deletion mutant (Fig. 5B), VP5, VP19C, VP23, and VP26 cosediment and are clearly evident beginning with fraction 8.

The sedimentation analysis of KUL26ΔZ-infected nonpermissive cells indicated that the peak of radioactivity which comprised capsid proteins VP5, VP19C, VP23, and VP26 was detected in fractions 11 and 12. To examine this more analytically, the radioactivity determined for each fraction was plotted as a function of the fraction number; the results are shown in Fig. 6. A peak of radioactivity was observed at fraction 11, which decreases rapidly at the higher fraction numbers but less rapidly in the fractions preceding 11. The

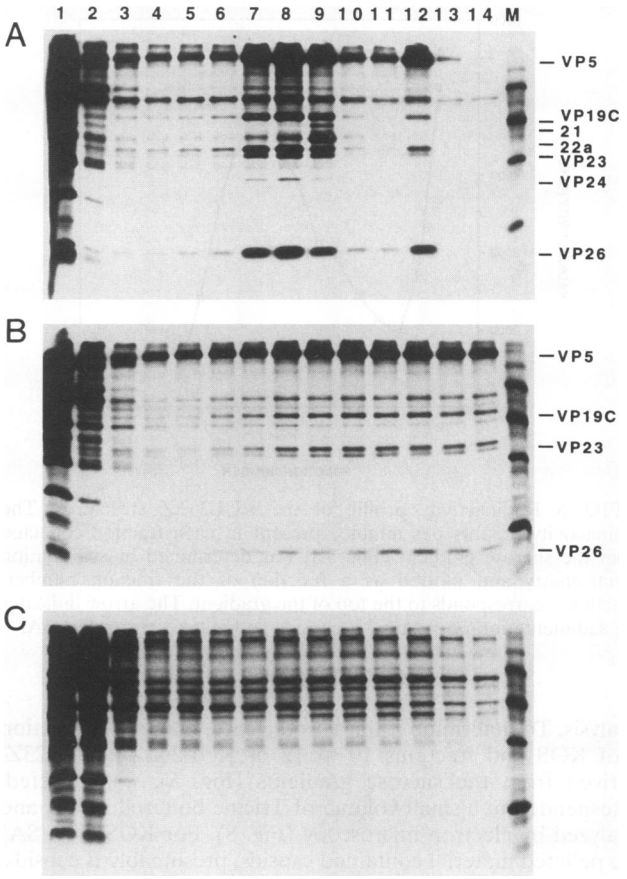

FIG. 5. Sedimentation analysis of nuclear lysates from infected HEL cells. HEL cells were infected with KOS (A), KUL26ΔZ (B), or K23Z (C) at an MOI of 10 PFU per cell. Cells were metabolically labeled with [^{35}S]methionine from 8 to 24 h postinfection. Nuclear lysates were layered onto 20 to 50% sucrose gradients and sedimented at 24,000 rpm for 100 min in a Beckman SW41 rotor. Fractions were collected, and proteins were analyzed by SDS-PAGE (17% polyacrylamide). The direction of sedimentation is from left to right. The mobilities of the capsid proteins are marked where observed. Protein molecular mass standards (97, 69, 46, 30, and 14 kDa) are shown in lane M.

peak of radioactivity sediments more rapidly than B capsids formed in KOS-infected cells (fraction 8). This was surprising and puzzling until material from these fractions was examined under the electron microscope.

Ultrastructural analysis of the UL26 null mutant. The UL26 null mutant was examined by electron microscopy to determine the nature of the structures detected by sedimentation analysis. Mutant and parental viruses were used to infect permissive and nonpermissive cells. At 12 h postinfection, samples were fixed in glutaraldehyde and the nuclei in tissue sections were examined by electron microscopy. The results are shown in Fig. 7. Capsids were detected in KOS-infected Vero cells (Fig. 7A) and in F3 cells infected with the UL26 null mutant (data not shown). Capsids were not observed in Vero cells infected with KUL26ΔZ (Fig. 7B). However, most of these tissue sections showed clusters of sheet-like aggregations. These aggregations were not evenly distributed throughout the nucleus but were localized to distinct regions; the aggregations may correspond to the structures detected by sedimentation

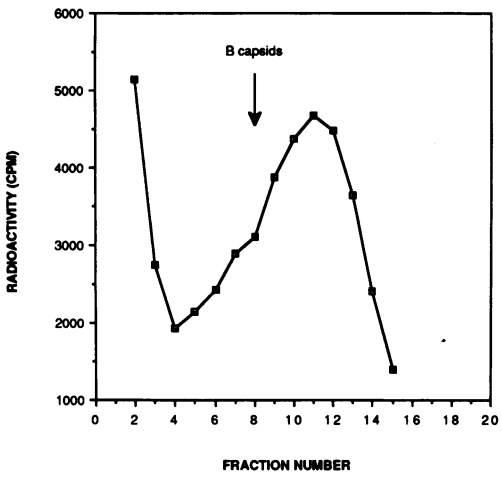

FIG. 6. Radioactivity profile of the KUL26ΔZ structures. The radioactivity (counts per minute) present in each fraction collected from the sucrose gradient (Fig. 5B) was determined by scintillation spectrometry and plotted as a function of the fraction number. Fraction 1 corresponds to the top of the gradient. The arrow indicates the sedimentation position of B capsids and is taken from Fig. 5A.

analysis. To determine if this was the case, material in fraction 8 of KOS and fractions 10 to 12 of KUL26ΔZ and K23Z, derived from the sucrose gradients (Fig. 5), was pelleted, resuspended in a small volume of Tricine-buffered saline, and analyzed by electron microscopy (Fig. 8). For KOS (Fig. 8A) the pelleted material contained capsids, presumably B capsids. In the case of the UL26 null mutant, sheet-like assembled structures of the capsid shell were observed (Fig. 8B); they appeared to be composed of organized capsomeres similar to those detected for wild-type capsids. Structures from mutant-infected cells were also stained with phosphotungstic acid and examined at somewhat higher magnifications (Fig. 8C). Large sheet and spiral structures are apparent. These are presumably capsid shells formed by extensive self-assembly of the subunits to yield structures much larger than B capsid shells. No structures were detected in the pelleted material derived from K23Z fractions (data not shown).

Chemical cross-linking of B capsids. Chemical cross-linking studies were undertaken to determine the spatial relatedness of the HSV-1 capsid proteins. Capsids from sucrose gradients were exposed to DSP, a cleavable homobifunctional cross-linker. It is amine reactive and may cross-link through the ε-amino group of lysine and possibly through the guanidino group of arginine and the imidizole group of histidine. The space between the reactive groups is 12 Å (1.2 nm) and contains a disulfide bond that is cleavable by exposure to a reducing agent. [^{35}S]methionine-labeled B capsids obtained after sedimentation through sucrose gradients were exposed to different concentrations of DSP (up to 0.33 mg/ml) for 30 min at room temperature. Cross-linking reactions were performed essentially as described by Rice and Strauss (37). One-dimensional SDS-PAGE analysis of the cross-linked proteins under nonreducing and reducing conditions revealed that as the concentration of DSP is increased, the individual capsid monomers disappear with the concomitant appearance of new cross-linked protein species (data not shown).

The composition of the cross-linked species was investigated by two-dimensional gel electrophoresis (Fig. 9). Capsid proteins were resolved in the first dimension in a 4 to 15% polyacrylamide gradient gel under nonreducing conditions and in the second dimension in a 17% gel under reducing conditions. A somewhat curved diagonal corresponding to un-cross-linked material is visible in capsids that were not exposed to DSP (Fig. 9A). It is evident that 22a must form disulfide-linked oligomers with itself since some of its radioactivity migrated more slowly than that of 22a monomers (to the right of the diagonal) in the nonreducing first dimension (Fig. 9A). In the presence of cross-linker, two distinct sets of cross-linked species are apparent (Fig. 9B). One is composed of VP5, VP19C, and 22a, and the second is composed of VP5, VP19C, and VP23. These complexes may reflect assembly intermediates that form during capsid morphogenesis.

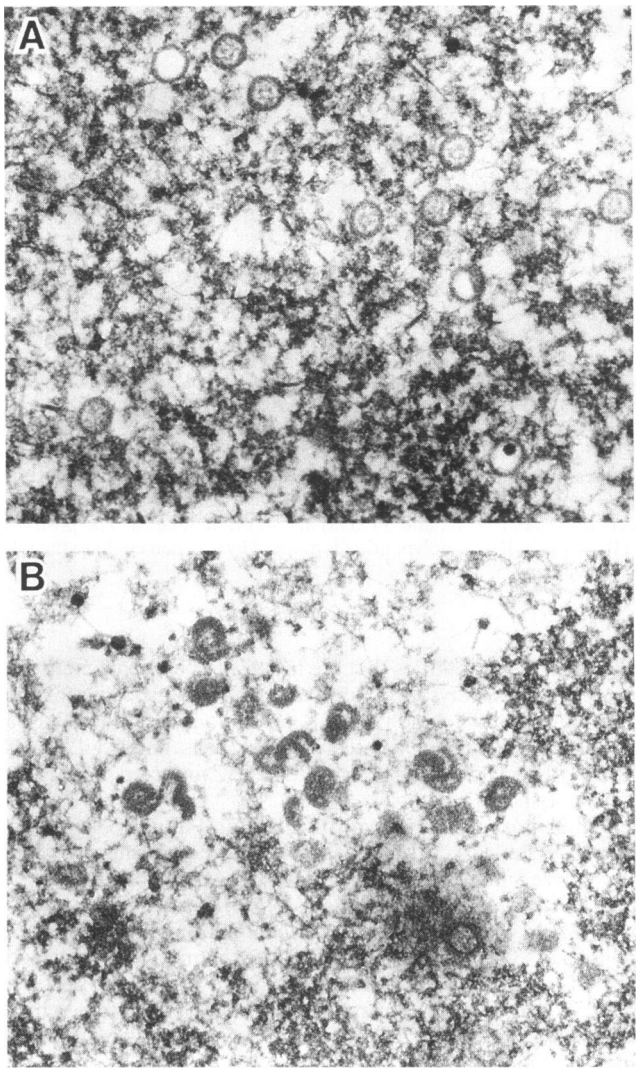

FIG. 7. Electron micrographs of thin sections of infected-cell nuclei. Monolayers of Vero cells were infected with KOS (A) and KUL26ΔZ (B) at an MOI of 10 PFU per cell. At 12 h postinfection, cells were fixed in 2.5% glutaraldehyde in phosphate-buffered saline and embedded in scipoxy 812 resin. Preparations were cut and stained with uranyl acetate (2%) and lead acetate (1%) and then examined in a JEOL 100 CX electron microscope. Magnification, ×48,500.

Proteolytic processing of 21 and 22a (ICP35) in the VP5 and VP23 null mutants. The suggested role for 21 and 22a is to form a scaffold which is essential for capsid assembly. The

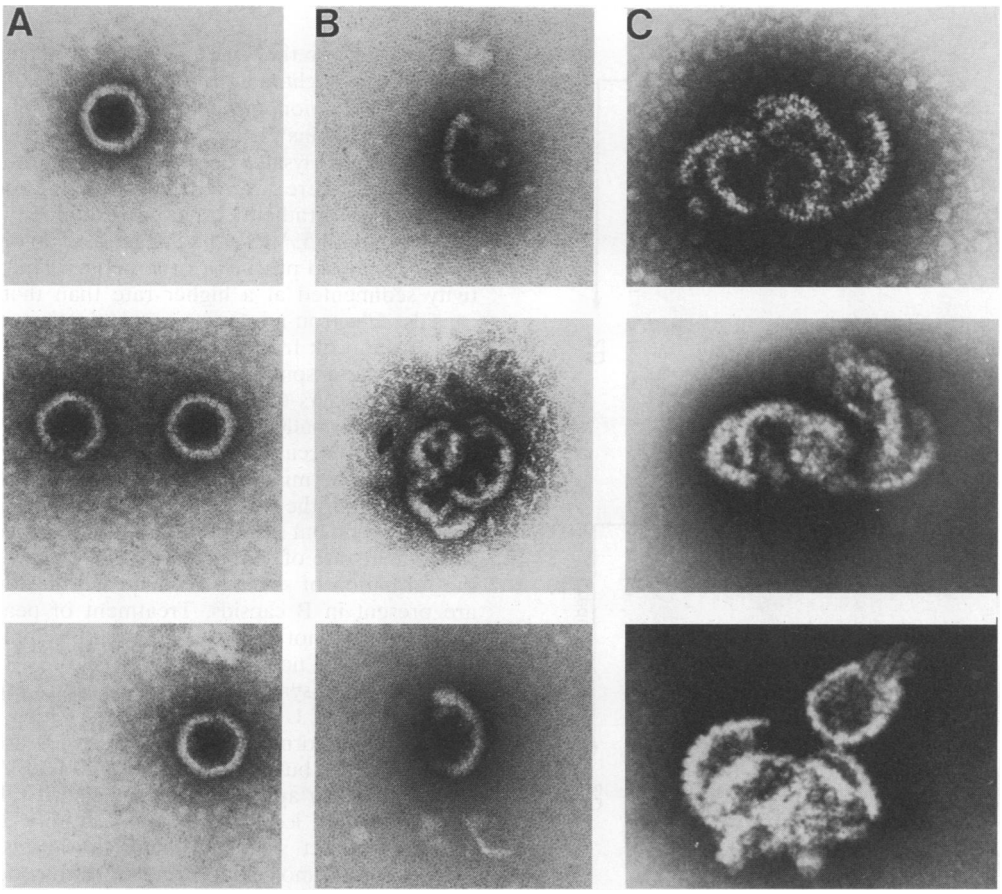

FIG. 8. Electron micrographs of negatively stained particles. Sucrose gradient fractions derived from the experiment shown in Fig. 5 were subjected to centrifugation, the pelleted material was resuspended in Tricine-buffered saline, and the particles were stained with uranyl acetate (A and B) or phosphotungstic acid (C) before electron microscopy. For KOS (A), particles in fraction 8 were pelleted; for KUL26ΔZ (B and C), fractions 10 to 12 were pelleted. Magnification, ×96,000 for panels A and B and ×115,000 (top), ×120,000 (middle), and ×150,000 (bottom) for panel C.

scaffold must also dissociate for packaging of viral DNA. Proteolytic cleavage of 21 and 22a at the maturation site (between amino acids 610 and 611) occurs at some stage during capsid assembly and may be related to scaffold dissociation. The question addressed in this section is whether the protease activity specified by the UL26 polypeptide is functional only in the context of an assembled capsid in virus-infected cells. Results from transient-expression studies suggest that this may not be the case (see, for example, references 7 and 46). The VP5 and VP23 null mutants are unable to form capsid-like structures or precursors in nonpermissive cells (10) and therefore offer an opportunity to address this question. HEL cells were infected with either KOS, K5ΔZ, or K23Z at an MOI of 10 PFU per cell. At 8 h postinfection the cells were either pulse-labeled with [^{35}S]methionine for 30 min or pulse-chase-labeled from 0.5 to 16 h after this time. Cell lysates from the infected cells were reacted with monoclonal antibody MCA406 (ICP35), and the resulting immunoprecipitates were analyzed by SDS-PAGE. The results (Fig. 10) indicate that all the UL26-specified polypeptides are expressed in mutant-infected cells (lanes 2 and 3). Furthermore, the ICP35 and the UL26 polypeptide are processed in K5ΔZ (lanes 2) and K23Z (lanes 3) extracts in a fashion similar to that seen in KOS-infected cells (lanes 1). The only discernible difference between wild-type- and mutant-infected cells is that the rate of processing is slightly lower for mutant-infected cells. One point of note is that more forms of ICP35 are detected in HEL-infected cells than in Vero cells; this may be related to the difference in the phosphorylating activities that may occur in these cells.

DISCUSSION

To obtain a mutant virus with a null mutation in UL26, it was necessary to isolate a transformed cell line that expresses the UL26 gene products, since it is known that at least one of these gene products is required for the production of infectious virions (14, 35). A 12.4-kb DNA fragment of HSV-1 (KOS) that encodes genes UL25 through UL28 (8) was used. Of a total of 37 stable G418-resistant transformants, 5 expressed the UL27 gene product (gB) at levels sufficient to support plaque formation of a gB null mutant virus (K082). Four of the five also supported the growth to the same extent of mutants with mutations in UL28 (KΔ4BX) and in UL26 (KUL26ΔZ). The cells were not checked for the expression of UL25. We previously transformed Vero cells with the 16.2-kb *Eco*RI G fragment, with similar results (10). The disadvantage of transformation of cells with large DNA fragments is that the probability of recombination between homologous sequences in viral and cellular DNA is proportionately increased.

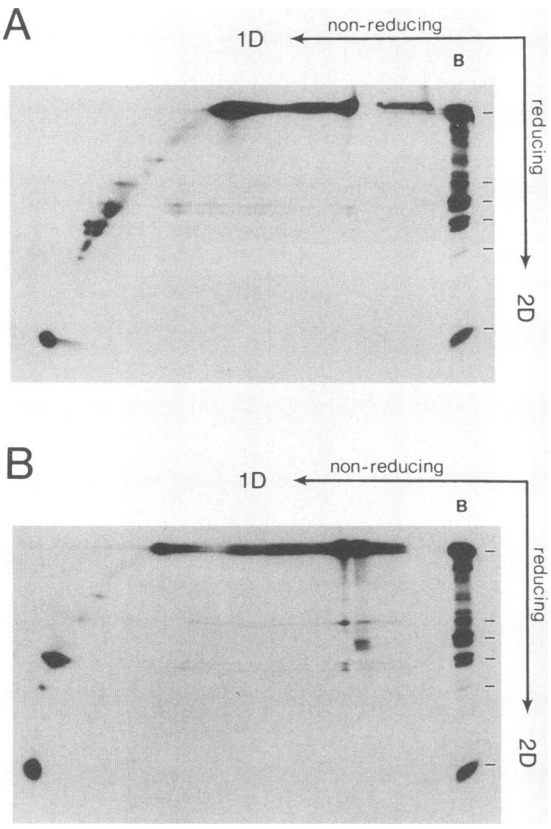

FIG. 9. Two-dimensional gel-electrophoretic analysis of cross-linked capsid proteins. [^{35}S]methionine-labeled B capsids, purified by sedimentation through sucrose gradients, were exposed to 0.33 mg of DSP per ml (B) or not exposed to DSP (A). Proteins were separated on a 4 to 15% polyacrylamide gradient gel in the first dimension (1D) (nonreducing) and on a 17% polyacrylamide gel in the second dimension (2D) (reducing), using a mini-protean gel apparatus. The gel slices from the first dimension were exposed to 1% SDS and 1% 2-mercaptoethanol in the stacking-gel buffer for 15 min at 65°C before separation in the second dimension was performed. Un-cross-linked B capsids were run in the lane marked B on the right side of the gel, and the positions of six capsid proteins corresponding to VP5, VP19C, 22a, VP23, VP24, and VP26 are marked.

Expression of the UL26 ORF was sufficient to allow the isolation and characterization of the null mutant virus, KUL26ΔZ. In nonpermissive cells, none of the UL26 gene products (proteins 21, 22a, and VP24) were expressed. Radiolabeled nuclear lysates derived from mutant-infected nonpermissive cells were layered on top of sucrose gradients and sedimented. Gradient fractions examined by SDS-PAGE showed that VP5, VP19C, VP23, and VP26 cosediment, indicative of a capsid precursor or structure. The peak of radioactivity sedimented at a higher rate than that of wild-type B capsids. Electron-microscopic examination of infected cells and of the peak fractions from the sucrose gradients showed sheet-like and spiral structures that appeared to be capsid shells. It appears that at least some of the weak interactions that occur normally between VP5, VP19C, VP23, and VP26 in capsids also occur in the shells observed in null-mutant-infected nonpermissive cells. These are sufficient to maintain the integrity of the capsid shell structure during extraction and sedimentation but insufficient to produce an icosahedral shape. The higher rate of sedimentation appears to be due partly to the formation of structures composed of more subunits than are present in B capsids. Treatment of peak fractions with DNase I did not affect the rate of sedimentation of the structures (data not shown).

The size and symmetry of B capsids are presumably due to the presence of UL26 gene products, which act as a scaffold during capsid formation. Since B capsids are formed in the presence of 22a but in the absence of 21 and VP24 (14, 44), the presence of 22a appears to be sufficient to determine capsid dimensions and icosahedral symmetry. For 22a molecules to give the correct size and shape to capsids, two physically distinct sets of molecular interactions may occur. One would be at the capsid shell and would be between 22a and VP5, VP19C, VP23, and/or VP26, which would cause the capsid to have the appropriate curvature. In the most simple model, the second set of interactions would be 22a self-interactions that give the spherical capsid the correct diameter. In the cross-linking data reported here and earlier by Zweig et al. (51), 22a was found to produce cross-links to itself; presumably, these are important during scaffold formation. Protein 22a also forms cross-links with VP5 and VP19C. These interactions may be essential during assembly of the capsid shell on the scaffold. Although cross-links to VP26 were not observed, VP26 does not contain lysine, one of the residues required for the cross-linking reaction used in this study. Cross-links between

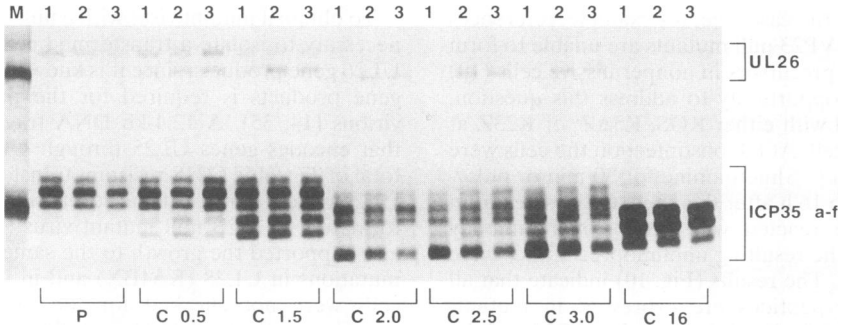

FIG. 10. Proteolytic cleavage of the UL26 and UL26.5 polypeptides. HEL cells were infected with KOS (lanes 1), K5ΔZ (lanes 2), and K23Z (lanes 3) at an MOI of 10 PFU per cell. Infected cells were pulse-labeled (P) with [^{35}S]methionine from 8 to 8.5 h postinfection or chased (C) thereafter for various times up to 16 h in the presence of cold methionine. Protein lysates prepared were reacted with a monoclonal antibody to ICP35 (MCA406; Serotec), and the resulting immunoprecipitates were analyzed by SDS-PAGE (9% polyacrylamide) on a standard Owl Scientific gel apparatus. Polypeptides corresponding to the full-length UL26 ORF and to the ICP35 a to f protein family are marked on the right of the gel. Protein standards corresponding to 69 and 46 kDa are shown in lane M.

VP5, VP19C, and VP23 were also detected, an interesting result in light of recent studies which suggest that VP19C and VP23 form the triplexes that link capsomeres in groups of three (31).

The results of the present experiments show that capsid shells of HSV-1 are composed mainly of VP5, VP19C, VP23, and VP26 and are consistent with a scaffold function for 22a. Molecular interactions among 22a molecules and between 22a and the molecules of the capsid shell determine capsid size and symmetry. Since capsid shells continue to enlarge in the absence of 22a, either the scaffold forms first or the shell and scaffold form concomitantly and capsid assembly proceeds outward from a sector. Although the present experiments address the question of capsid formation, they provide no information on the initiation or termination events required for capsid assembly.

It is interesting to speculate on the arrangement of 22a in capsids and on the role of the protease specified by UL26. The interactions of 22a with other capsid proteins may involve the C-terminal residues of 22a. Perhaps those residues are not available for cleavage by the protease (VP24) until B capsids are completed, when conformation changes expose the cleavage sites. Since the cleaved form of 22a appears to be the major form present in B capsids, cleavage appears to be temporally separated from DNA packaging (40, 46). Protease processing also occurs in the absence of VP5 and VP23 and, consequently, of capsid formation. Therefore, if the enzyme and substrate are expressed together and come into contact, cleavage will occur. This is also consistent with results of transient-expression assays with bacterial and mammalian cells (7, 25, 46). Although enzyme activity is independent of structure, this may not accurately reflect the role of the UL26 gene products in capsid formation and maturation. Further experiments are required to determine the functional requirements of the protease in viral infections.

Mutants with null mutations in VP5 and in VP23 (10), as well as mutants with temperature-sensitive mutations in VP5 (39) and in VP19C (34) have the same phenotype; no discernible structures are produced under nonpermissive conditions. Data are needed for mutants with null mutations in VP19C and in VP26 to determine if these proteins play an integral role in the assembly of the capsid shell. Thomsen et al. (44) have recently reported capsid formation by expression of cloned gene products in insect cells infected with recombinant baculovirus. Deletion of UL26 gene products (proteins 21 and VP24) gave rise to B capsids, whereas deletion of UL26.5 (protein 22a) produced capsids that appeared to lack a proteinaceous core. This implies that protein 21 produced in sufficient quantity can replace protein 22a to some extent to give capsids their correct symmetry. Capsid shells similar to those reported here were found when 21, 22a, VP24, and VP26 were absent, which could indicate that VP26 is not essential for the formation of a shell structure. However, in their system, capsids were formed in the absence of VP23, a result that was not obtained following infection of nonpermissive cells with a mutant with a null mutation in the VP23 gene (10). This may reflect differences in expression or posttranslational processing of the capsid proteins in the baculovirus-insect cell system. However, the results of the two quite different experiments, i.e., that a capsid shell composed mainly of VP5, VP19C, VP23, and VP26 is normally formed by accretion on a scaffold of 22a, are in agreement.

One of the most common pathways of capsid assembly of complex bacteriophage heads includes the formation of a centrally located molecular structure, termed the scaffold, which is present in capsids but not in mature phages. Although viruses with small genomes can self-assemble directly from a pool of molecules that are present in mature virus particles, viruses with larger genomes may require the presence of accessory proteins, including scaffolding proteins, to catalyze assembly (21). Scaffold proteins have been reported for *Salmonella typhimurium* bacteriophage P22, for *Bacillus subtilis* phage ϕ29, and for coliphages λ, T3, T4, and T7 among others (see, for example, reference 50). The presence of the scaffold protein is reciprocally related to the presence of DNA during capsid maturation. In the case of λ head assembly, the scaffold protein is removed from the head structure prior to the entry of DNA. Protease cleavage of the scaffold protein is not a prerequisite for DNA packaging. For example, the gp8 scaffold protein of P22 is released intact and reused in the formation of other bacteriophage heads. The scaffold, through interactions with the proteins of the capsid shell and possibly with itself, determines the size and symmetry of the capsid. Since the space vacated by the scaffold is subsequently filled with DNA, the size of the scaffold determines the amount of DNA that can be packaged into the capsid (21). The formation of HSV-1 B capsids reported here is entirely analogous to the assembly of the heads of many bacteriophages, and giant structures similar to those observed here were reported for a scaffold protein (gp8) mutant of P22 (22). It is interesting that the same general strategy, with relatively minor variations, is used for viral capsid formation in prokaryotes and eukaryotes.

ACKNOWLEDGMENTS

This work was supported by Public Health Service grant AI33077 from the National Institutes of Health.

It is a pleasure to acknowledge discussion of data with Neal A. DeLuca.

REFERENCES

1. **Baker, T. S., W. W. Newcomb, F. P. Booy, J. C. Brown, and A. C. Steven.** 1990. Three-dimensional structures of maturable and abortive capsids of equine herpesvirus 1 from cryoelectron microscopy. J. Virol. **64**:563–573.
2. **Braun, D. K., B. Roizman, and L. Pereira.** 1984. Characterization of post-translational products of herpes simplex virus gene 35 proteins binding to the surfaces of full but not empty capsids. J. Virol. **49**:142–153.
3. **Cai, W., S. Person, S. C. Warner, J. Zhou, and N. A. DeLuca.** 1987. Linker-insertion nonsense and restriction-site deletion mutations of the gB glycoprotein gene of herpes simplex virus type 1. J. Virol. **61**:714–721.
4. **Chakrabarti, S., K. Brechling, and B. Moss.** 1985. Vaccinia virus expression vector: coexpression of β-galactosidase provides a visual screening of recombinant plaques. Mol. Cell. Biol. **5**:3403–3409.
5. **Cohen, G. H., M. Ponce de Leon, H. Diggleman, W. C. Lawrence, S. K. Vernon, and R. J. Eisenberg.** 1980. Structural analysis of the capsid polypeptides of herpes simplex virus types 1 and 2. J. Virol. **34**:521–531.
6. **Davison, M. D., F. J. Rixon, and A. J. Davison.** 1992. Identification of genes encoding two capsid proteins (VP24 and VP26) of herpes simplex virus type 1. J. Gen. Virol. **73**:2709–2713.
7. **Deckman, I. C., M. Hagen, and P. J. McCann.** 1992. Herpes simplex virus type 1 protease expressed in *Escherichia coli* exhibits autoprocessing and specific cleavage of the ICP35 assembly protein. J. Virol. **66**:7362–7367.
8. **DeLuca, N., D. J. Bzik, V. C. Bond, S. Person, and W. Snipes.** 1982. Nucleotide sequences of herpes simplex virus type 1 (HSV-1) affecting virus entry, cell fusion, and production of glycoprotein B (VP7). Virology **122**:411–423.
9. **DeLuca, N. A., A. M. McCarthy, and P. A. Schaffer.** 1985. Isolation and characterization of deletion mutants of herpes simplex virus type 1 in the gene encoding immediate-early regulatory protein ICP4. J. Virol. **56**:558–570.
10. **Desai, P., N. A. DeLuca, J. C. Glorioso, and S. Person.** 1993. Mutations in herpes simplex virus type 1 genes encoding VP5 and VP23 abrogate capsid formation and cleavage of replicated DNA. J. Virol. **67**:1357–1364.

11. **Desai, P., F. L. Homa, S. Person, and J. C. Glorioso.** A genetic selection method for the transfer of HSV-1 glycoprotein B mutations from plasmid to the viral genome: the transdominance and entry kinetics of mutant viruses. Submitted for publication.
12. **Dilanni, C. L., D. A. Drier, I. C. Deckman, P. J. McCann, F. Liu, B. Roizman, R. J. Colonno, and M. G. Cordingly.** 1993. Identification of the herpes simplex virus-1 protease cleavage sites by direct sequence analysis of autoproteolytic cleavage products. J. Biol. Chem. **268:**2048–2051.
13. **Feinberg, A. P., and B. Vogelstein.** 1984. A technique for radiolabeling DNA restriction fragments to high specific activity. Anal. Biochem. **137:**6–13.
14. **Gao, M., L. Matusick-Kumar, W. Hurlburt, S. F. DiTusa, W. W. Newcomb, J. C. Brown, P. J. McCann, I. Deckman, and R. J. Colonno.** 1994. The protease of herpes simplex virus type 1 is essential for functional capsid formation and viral growth. J. Virol. **68:**3702–3712.
15. **Gibson, W., A. I. Marcy, J. C. Comolli, and J. Lee.** 1990. Identification of precursor to cytomegalovirus capsid assembly protein and evidence that processing results in loss of its carboxy-terminal end. J. Virol. **64:**1241–1249.
16. **Gibson, W., and B. Roizman.** 1972. Proteins specified by herpes simplex virus. VIII. Characterization and composition of multiple capsid forms of subtypes 1 and 2. J. Virol. **10:**1044–1052.
17. **Gibson, W., and B. Roizman.** 1974. Proteins specified by herpes simplex virus. X. Staining and radiolabeling properties of B capsid and virion proteins in polyacrylamide gels. J. Virol. **13:**155–165.
18. **Graham, F. L., and A. J. van der Eb.** 1973. A new technique for the assay of infectivity of human adenovirus 5 DNA. Virology **52:**456–467.
19. **Heilman, C. J., M. Zweig, J. R. Stephenson, and B. Hampar.** 1979. Isolation of a nucleocapsid polypeptide of herpes simplex virus types 1 and 2 possessing immunologically type-specific and cross-reactive determinants. J. Virol. **29:**34–42.
20. **Holland, L. E., R. M. Sandri-Goldin, A. L. Goldin, J. C. Glorioso, and M. Levine.** 1984. Transcriptional and genetic analyses of the herpes simplex virus type 1 genome: coordinates 0.29 to 0.45. J. Virol. **49:**947–959.
21. **King, J., and S. Casjens.** 1974. Catalytic head assembling protein in virion morphogenesis. Nature (London) **251:**112–119.
22. **King, J., E. V. Lenk, and D. Botstein.** 1973. Mechanism of head assembly and DNA encapsulation in *Salmonella* phage P22. J. Mol. Biol. **80:**697–731.
23. **Liu, F., and B. Roizman.** 1991. The promoter, transcriptional unit, and coding sequences of the herpes simplex virus 1 family 35 proteins are contained within and in frame with the UL26 open reading frame. J. Virol. **65:**206–212.
24. **Liu, F., and B. Roizman.** 1993. Characterization of the protease and other products of amino-terminus-proximal cleavage of the herpes simplex virus 1 U_L26 protein. J. Virol. **67:**1300–1309.
25. **Liu, F. Y., and B. Roizman.** 1991. The herpes simplex virus type 1 gene encoding a protease also contains within its coding domain the gene encoding the more abundant substrate. J. Virol. **65:**5149–5156.
26. **McGeoch, D. J., M. A. Dalrymple, A. J. Davison, A. Dolan, M. C. Frame, D. McNab, L. J. Perry, J. E. Scott, and P. Taylor.** 1988. The complete DNA sequence of the long unique region in the genome of herpes simplex virus type 1. J. Gen. Virol. **69:**1531–1574.
27. **McGeoch, D. J., S. K. Weller, and P. A. Schaffer.** 1990. Herpes simplex virus, p. 1.115–1.120. *In* S. J. O'Brien (ed.), Genetic maps. Cold Spring Harbor Laboratory Press, Cold Spring Harbor, N.Y.
28. **Newcomb, W. W., and J. C. Brown.** 1989. Use of Ar^+ plasma etching to localize structural proteins in the capsid of herpes simplex virus type 1. J. Virol. **63:**4697–4702.
29. **Newcomb, W. W., and J. C. Brown.** 1991. Structure of the herpes simplex virus capsid: effects of extraction with guanidine hydrochloride and partial reconstitution of extracted capsids. J. Virol. **65:**613–620.
30. **Newcomb, W. W., J. C. Brown, F. P. Booy, and A. C. Steven.** 1989. Nucleocapsid mass and capsomer protein stoichiometry in equine herpesvirus 1: a scanning transmission electron microscopic study. J. Virol. **63:**3777–3783.
31. **Newcomb, W. W., B. L. Trus., F. P. Booy, A. C. Steven, J. S. Wall, and J. C. Brown.** 1993. Structure of the herpes simplex virus capsid: molecular composition of the pentons and the triplexes. J. Mol. Biol. **232:**499–511.
32. **Person, S., R. W. Knowles, G. S. Read, S. C. Warner, and V. C. Bond.** 1976. Kinetics of cell fusion induced by a syncytia-producing mutant of herpes simplex virus type I. J. Virol. **17:**183–190.
33. **Person, S., S. Laquerre, P. Desai, and J. Hempel.** 1993. Herpes simplex virus type 1 capsid protein, VP21, originates within the UL26 open reading frame. J. Gen. Virol. **74:**2269–2273.
34. **Pertuiset, B., M. Boccara, J. Cebrian, N. Berthelot, S. Chousterman, F. Puvion-Dutilleul, J. Sisman, and P. Sheldrick.** 1989. Physical mapping and nucleotide sequence of a herpes simplex virus type 1 gene required for capsid assembly. J. Virol. **63:**2169–2179.
35. **Preston, V. G., J. A. V. Coates, and F. J. Rixon.** 1983. Identification and characterization of a herpes simplex virus gene product required for encapsidation of virus DNA. J. Virol. **45:**1056–1064.
36. **Preston, V. G., F. J. Rixon, I. M. McDougall, M. McGregor, and M. F. Al Kobaisi.** 1992. Processing of the herpes simplex virus assembly protein ICP35 near its carboxy terminal end requires the product of the whole of the UL26 reading frame. Virology **186:**87–98.
37. **Rice, C. M., and J. H. Strauss.** 1982. Association of Sindbis virion glycoproteins and their precursors. J. Mol. Biol. **154:**325–348.
38. **Rixon, F. J., A. M. Cross, C. Addison, and V. G. Preston.** 1988. The products of the herpes simplex virus type 1 gene UL26 which are involved in DNA packaging are strongly associated with empty but not with full capsids. J. Gen. Virol. **69:**2879–2891.
39. **Schaffer, P. A., J. P. Brunschwig, R. M. McCombs, and M. Benyesh-Melnick.** 1974. Electron microscopic studies of temperature-sensitive mutants of herpes simplex virus type 1. Virology **62:**444–457.
40. **Schenk, P., A. S. Woods, and W. Gibson.** 1991. The 45-kilodalton protein of cytomegalovirus (Colburn) B-capsids is an amino-terminal extension form of the assembly protein. J. Virol. **65:**1525–1529.
41. **Southern, E. M.** 1975. Detection of specific sequences among DNA fragments separated by gel electrophoresis. J. Mol. Biol. **98:**503–517.
42. **Southern, P. J., and P. Berg.** 1982. Transformation of mammalian cells to antibiotic resistance with a bacterial gene under the control of the SV40 early region promoter. J. Mol. Appl. Genet. **1:**327–341.
43. **Spear, P. G., and B. Roizman.** 1972. Proteins specified by herpes simplex virus. V. Purification and structural proteins of the herpesvirion. J. Virol. **9:**143–159.
44. **Thomsen, D. R., L. L. Roof, and F. L. Homa.** 1994. Assembly of herpes simplex virus (HSV) intermediate capsids in insect cells infected with recombinant baculoviruses expressing HSV capsid proteins. J. Virol. **68:**2442–2457.
45. **Vernon, S. K., M. Ponce de Leon, G. H. Cohen, R. J. Eisenberg, and B. A. Rubin.** 1981. Morphological components of herpesvirus. III. Localization of herpes simplex virus type 1 nucleocapsid polypeptides by immune electron microscopy. J. Gen. Virol. **54:**39–46.
46. **Weinheimer, S. P., P. J. McCann, D. R. O'Boyle, J. T. Stevens, B. A. Boyd, D. A. Drier, G. A. Yamanaka, C. L. Dilanni, I. C. Deckman, and M. G. Cordingly.** 1993. Autoproteolysis of herpes simplex virus type 1 protease releases an active catalytic domain found in intermediate capsid particles. J. Virol. **67:**5813–5822.
47. **Welch, A. R., L. M. McNally, M. R. T. Hall, and W. Gibson.** 1993. Herpesvirus proteinase: site-directed mutagenesis used to study maturational, release, and inactivation cleavage sites of precursor and to identify a possible catalytic site serine and histidine. J. Virol. **67:**7360–7372.
48. **Welch, A. R., A. S. Woods, L. M. McNally, R. J. Cotter and W. Gibson.** 1991. A herpesvirus maturational proteinase, assemblin: identification of its gene, putative active site, and cleavage site. Proc. Natl. Acad. Sci. USA **88:**10792–10796.
49. **Wildy, P., W. C. Russell, and R. W. Horne.** 1960. The morphology of herpes virus. Virology **12:**204–222.
50. **Wood, W. B., and J. King.** 1979. Genetic control of complex bacteriophage assembly, p. 581–633. *In* H. Fraenkal-Conrat and R. R. Wagner (ed.), Comprehensive virology, vol. 13. Plenum Press, New York.
51. **Zweig, M., C. J. Heilman, and B. Hampar.** 1979. Identification of disulfide-linked protein complexes in the nucleocapsids of herpes simplex type 2. Virology **94:**442–450.